

Limits on Dark Radiation, Early Dark Energy, and Relativistic Degrees of Freedom

Erminia Calabrese¹, Dragan Huterer², Eric V. Linder^{3,4}, Alessandro Melchiorri¹, Luca Pagano⁵

¹ *Physics Department and INFN, Università di Roma “La Sapienza”, Ple Aldo Moro 2, 00185, Rome, Italy.*

² *Department of Physics, University of Michigan, 450 Church St, Ann Arbor, MI 48109, USA.*

³ *Berkeley Lab & University of California, Berkeley, CA 94720, USA.*

⁴ *Institute for the Early Universe WCU, Ewha Womans University, Seoul, Korea and*

⁵ *Jet Propulsion Laboratory, California Institute of Technology,
4800 Oak Grove Drive, Pasadena CA 91109, USA.*

Recent cosmological data analyses hint at the presence of an extra relativistic energy component in the early universe. This component is often parametrized as an excess of the effective neutrino number N_{eff} over the standard value of 3.046. The excess relativistic energy could be an indication for an extra (sterile) neutrino, but early dark energy and barotropic dark energy also contribute to the relativistic degrees of freedom. We examine the capabilities of current and future data to constrain and discriminate between these explanations, and to detect the early dark energy density associated with them. We find that while early dark energy does not alter the current constraints on N_{eff} , a dark radiation component, such as that provided by barotropic dark energy models, can substantially change current constraints on N_{eff} , bringing its value back to agreement with the theoretical prediction. Both dark energy models also have implications for the primordial mass fraction of Helium Y_p and the scalar perturbation index n_s . The ongoing Planck satellite mission will be able to further discriminate between sterile neutrinos and early dark energy.

I. INTRODUCTION

The precision of theoretical modelling and observational measurements of the cosmic microwave background (CMB) temperature and polarization anisotropies from satellites and ground based experiments [1–4] has opened the exciting possibility of addressing key questions about the nature of dark energy, dark matter and primordial inflation. Interestingly, a first hint of some new physics may be showing up in the high redshift universe from CMB and Big Bang nucleosynthesis (BBN) data. Recent analyses (for example [1, 4–7]) may be hinting at the need for an extra, dark, relativistic energy component.

If further data confirms this, it could suggest new dark matter such as a sterile neutrino [5] or a decaying particle [8–10], or nonstandard thermal history [11]. Or it could indicate that dark energy does not fade away to the $\sim 10^{-9}$ fraction of the energy density at CMB recombination that is predicted by the cosmological constant. Indeed, some proposed particle physics explanations for dark energy involve scaling fields [12, 13] with an early energy density which is a constant fraction of the energy density of the dominant component. Another possibility is that the evidence for the extra relativistic component may be signaling the presence of a “dark radiation” component in the early universe, as predicted by certain higher dimension braneworld scenarios [14].

Any of these would be exciting extensions to the standard, concordance model. Uncovering new degrees of freedom would be of great importance, and distinguishing between the possible origins could give valuable insight into physics and cosmology. The extra, dark contribution to the total relativistic energy density in the early Universe is generally phrased in terms of the energy density of neutrinos – the known dark, (early) relativistic com-

ponent. One defines the effective number of neutrinos N_{eff} through :

$$\rho_\nu = \rho_\gamma \frac{7}{8} \left(\frac{4}{11} \right)^{4/3} N_{\text{eff}} , \quad (1)$$

where ρ_ν is the neutrino energy density and ρ_γ is the CMB photon energy density, with value today $\rho_{\gamma,0} \approx 4.8 \times 10^{-34} \text{ g cm}^{-3}$. In the standard model, with three massless neutrinos with zero chemical potential and in the limit of instantaneous decoupling, $N_{\text{eff}} = 3$. The inclusion of entropy transfer between neutrinos and the thermal bath modifies this number to about $N_{\text{eff}} = 3.046$ at the CMB epoch (see e.g. [6]).

The recent analysis of [4] that combined CMB data with measurements of baryon acoustic oscillations (BAO) and the Hubble constant reported an excess of the relativistic neutrino number, $N_{\text{eff}} = 4.6 \pm 0.8$ at 68% c.l., disfavoring the standard value at about two standard deviations. This is compatible with previous analyses [1, 5–7].

Another possible high redshift discrepancy, also sensitive to relativistic degrees of freedom, involves primordial ^4He measurements compared with the predictions of Big Bang nucleosynthesis (see, e.g., [5, 15]). While standard BBN, assuming a value of the baryon-photon ratio of $\eta = (6.19 \pm 0.15) \times 10^{-10}$ as measured by CMB data [1], predicts a primordial Helium mass fraction $Y_p = 0.2487 \pm 0.0002$, current observational measurements prefer a larger value of $Y_p = 0.2561 \pm 0.0108$ [16] and $Y_p = 0.2565 \pm 0.0010(\text{stat.}) \pm 0.0050(\text{syst.})$ [17]. Since the primordial ^4He mass fraction is largely determined by the neutron to proton ratio at the start of BBN, Y_p is sensitive to the value of the expansion rate and so through the Friedmann equation to the overall energy density at temperature $\sim 1 \text{ MeV}$, e.g. in relativistic particles. From [18] one has approximately $\Delta Y_p \simeq 0.013(N_{\text{eff}} - 3)$ for

$|N_{\text{eff}} - 3| \lesssim 1$. Thus, an increase in the effective number of relativistic degrees of freedom could remove the tension between BBN and the measured ^4He abundances.

These new relativistic degrees of freedom (RDOF) could be due, for example, to a fourth (or fifth), sterile neutrino (a postulated neutrino species that does not participate in weak interactions). Such a hypothesis is worthwhile testing and may also be compatible with recent neutrino oscillation results (e.g. [19–21]). This origin would have no direct relation to the question of cosmic acceleration and dark energy.

However, the signal could also arise from the class of early dark energy models. Scalar fields from dilatons in field theory and moduli in string theory are generally predicted to possess scaling properties, so that they would evolve as radiation in the radiation dominated era and contribute a constant fraction of energy density. Extending probes of dark energy to high redshift is an important frontier and detection of its effects would provide an invaluable guide to the physics behind cosmic acceleration. Dark energy that is significantly present not only in the late universe but also at early times is called early dark energy (EDE; see, e.g., [22, 23]). Furthermore, some theories, typically involving higher dimensions, predict a “dark radiation” component in addition to a cosmological constant.

All three origins increase RDOF but have different evolutions in the energy density as radiation domination wanes, and hence will have the expansion history and N_{eff} differing as a function of time. In this paper we consider the effects of contributions to N_{eff} from both neutrino and dark energy components, individually and together, and analyse the constraints imposed by current and future cosmological data. The main motivations are 1) to investigate how the current indication for RDOF would translate into a signal for dark energy at high redshift, and 2) to examine how adopting a dark energy component that is not negligible at high redshift would impact the stability of future possible conclusions from Planck about RDOF.

As a product of this analysis, we update the current constraints on EDE with recent data. Previous analysis have placed constraints on EDE using the available cosmological datasets and forecasting the discriminatory power of future CMB probes like Planck (see e.g. [24–28]). Here we revise these constraints by using updated datasets, by enlarging the parameter space through including shear viscosity in EDE perturbations, and by considering the possible degeneracies with sterile neutrinos. Section II describes in more detail the models used to give extra N_{eff} . In Sec. III we present the results of our analysis for the different cases, and Sec. IV discusses the conclusions about the ability to constrain and distinguish the various physical origins.

II. NEUTRINOS, EARLY DARK ENERGY, AND DARK RADIATION

We consider three models that contribute to RDOF: sterile neutrinos, early dark energy, and a barotropic dark energy model that produces a dark radiation component in the early universe. Accounting for each possible contribution, the RDOF translated into an effective number of neutrinos is :

$$N_{\text{eff}} = N_{\text{eff}}^{\nu} + \Delta N_{\text{eff}}^{\text{EDE}} + \Delta N_{\text{eff}}^{\text{B}} , \quad (2)$$

where N_{eff}^{ν} is the number of neutrino species (including extra sterile neutrinos), $\Delta N_{\text{eff}}^{\text{EDE}}$ is the contribution coming from early dark energy, and $\Delta N_{\text{eff}}^{\text{B}}$ is the contribution from barotropic dark energy. When the components do not behave completely relativistically, the effective numbers may be functions of redshift; for EDE the contribution is constant only well before matter-radiation equality, while barotropic dark energy behaves as a relativistic component at all times during and before recombination. In the following sections we describe our modelling for these three components and then their physical signatures in CMB power spectra, before proceeding to the ability of cosmological data to constrain and discriminate among them.

A. Relativistic Neutrinos

For the purposes of exploring a deviation from the standard value of $N_{\text{eff}} = 3.046$, we first assume thermal (so the factors in Eq. (1) hold), massless sterile neutrinos which give a time-independent contribution to N_{eff} according to Eq. (1). We indicate the total neutrino contribution to N_{eff} by N_{eff}^{ν} , which is not necessarily equal to N_{eff} any more. Current cosmological data bound the mass of extra (thermal) sterile neutrinos to be $m_{\nu,s} \lesssim 0.5 \text{ eV}$ for $N_{\text{eff}} \geq 4$ at 95% c.l. ([5, 29]). Such massive sterile neutrinos may also be compatible with recent neutrino oscillation results (e.g. [19–21]), however considering them as massive has negligible impact on the constraints on N_{eff} (again, see [29]) and we treat these neutrinos as massless in what follows. Neutrinos with $\sim \text{keV}$ masses, sometimes considered for sterile neutrinos, are non-relativistic at recombination and contribute little to N_{eff} at that time. Note that, while we refer N_{eff}^{ν} to sterile neutrinos in what follows, other relativistic backgrounds (for example, gravitational waves) produce identical effects on cosmology. See [30] for a decaying particle scenario. Any such model that lacks significant contribution to late time energy density is for our purposes equivalent to sterile neutrinos.

The usual case, e.g. in [4], is to analyze the constraints on N_{eff}^{ν} in the absence of an early dark energy density, in which case $N_{\text{eff}} = N_{\text{eff}}^{\nu}$. We consider in this article N_{eff}^{ν} in the presence of an early dark energy density.

B. Early Dark Energy

Early dark energy is the name given to a dark component that in the recent universe acts to accelerate expansion, but which retains a non-negligible energy density at early times (e.g. around recombination, or earlier). To keep an appreciable energy density at early times, the equation of state would not be negative, but at or near that of the background equation of state. We adopt the commonly used form [22]

$$\Omega_{\text{de}}(a) = \frac{\Omega_{\text{de}}^0 - \Omega_e (1 - a^{-3w_0})}{\Omega_{\text{de}}^0 + \Omega_m^0 a^{3w_0}} + \Omega_e (1 - a^{-3w_0}) \quad (3)$$

$$w(a) = -\frac{1}{3[1 - \Omega_{\text{de}}(a)]} \frac{d \ln \Omega_{\text{de}}(a)}{d \ln a} + \frac{a_{\text{eq}}}{3(a + a_{\text{eq}})} \quad (4)$$

where $\Omega_{\text{de}}(a)$ is the fractional energy density and $w(a)$ the equation of state of EDE. The factor $a_{\text{eq}}/(a + a_{\text{eq}})$ in Eq. (4) comes from $\Omega_r(a)/[1 - \Omega_{\text{de}}(a)]$ where Ω_r is the fractional radiation energy density (specifically excluding any EDE) and a_{eq} is the scale factor at matter-radiation equality. Here Ω_{de}^0 and Ω_m^0 are the current dark energy and matter density, respectively, and a flat Universe is assumed so $\Omega_m^0 + \Omega_{\text{de}}^0 = 1$. The present equation of state $w(a=1) = w_0$. The energy density $\Omega_{\text{de}}(a)$ goes to a finite constant Ω_e in the past, in both the matter dominated and radiation dominated eras, indicating a scaling solution.

The dark energy equation of state $w(a)$ follows three distinct behaviours: $w \approx 1/3$ during radiation domination, $w \approx 0$ during matter domination, and $w \approx w_0$ in recent epochs. An accurate fitting formula for the time variation of the EDE equation of state during the recent universe is $w_a = 5\Omega_e$ [23], where $w(a) = w_0 + w_a(1 - a)$ fits observational quantities at $z < 3$ to 0.1% accuracy. We extend the model by modeling the EDE clustering properties through the effective sound speed $c_s^2 = \delta p / \delta \rho$ and a viscosity parameter c_{vis}^2 that describes the possible presence of anisotropic stresses (see e.g. [24] and references therein). In what follows we assume these clustering parameters as constant and consider two cases: $c_s^2 = c_{\text{vis}}^2 = 1/3$, corresponding to a relativistic origin, and $c_s^2 = 1$, $c_{\text{vis}}^2 = 0$ as expected in the case of a quintessence scalar field. For simplicity we consider $w_0 = -1$ since the low redshift data are consistent with a cosmological constant and viable EDE models have little time variation there.

Regarding the contribution to N_{eff} , the EDE scaling behavior indicates the energy density will behave as a relativistic component until the epoch of matter-radiation equality and so $\Delta N_{\text{eff}}^{\text{EDE}}$ will be constant by Eq. (1). However, since w then deviates from $1/3$ toward 0 as the EDE later behaves more non-relativistically, $\Delta N_{\text{eff}}^{\text{EDE}}$ will grow. Translating the EDE density into an effective “neutrino” number $\Delta N_{\text{eff}}^{\text{EDE}}$ through Eq. (1) yields :

$$\Delta N_{\text{eff}}^{\text{EDE}}(a) = \left[\frac{7}{8} \left(\frac{4}{11} \right)^{4/3} \right]^{-1} \frac{\rho_{\text{de}}(a)}{\rho_{\gamma}(a)}. \quad (5)$$

This is clearly a redshift-dependent quantity since as the EDE equation of state begins to evolve differently from radiation the density ratio will vary with time. In the limit $a \ll a_{\text{eq}}$,

$$\Delta N_{\text{eff}}^{\text{EDE}}(a \ll a_{\text{eq}}) = 7.44 \frac{\Omega_e}{1 - \Omega_e}, \quad (6)$$

since $\rho_{\text{de}}/\rho_{\gamma} = (\rho_{\text{de}}/\rho_{\text{rad}})(\rho_{\text{rad}}/\rho_{\gamma})$ and $\rho_{\text{rad}}/\rho_{\gamma} = 1.69$ for three neutrino species.

In Figure 1 we plot $\Delta N_{\text{eff}}^{\text{EDE}}(a)$, for $\Omega_e = 0.05$. As we can see, at early times EDE behaves like a RDOF component with a constant value of $\Delta N_{\text{eff}}^{\text{EDE}} \approx 0.39$. However this value increases at later times, when EDE starts to mutate into a matter-scaling component, reaching $\Delta N_{\text{eff}}^{\text{EDE}} \approx 1.6$ at recombination. This time dependence will be a crucial element in discriminating between EDE and a sterile neutrino contribution N_{eff}^{ν} . Having ΔN_{eff} in EDE models smaller at BBN than at recombination helps ease the discrepancy between the lower value expected (3.046) and that derived from CMB data. Furthermore, the larger value of ΔN_{eff} at recombination means that the constraints on EDE from CMB anisotropies will translate to tighter bounds on $\Delta N_{\text{eff}}^{\text{EDE}}$ at BBN, and hence on Y_p , than those in the neutrino RDOF case.

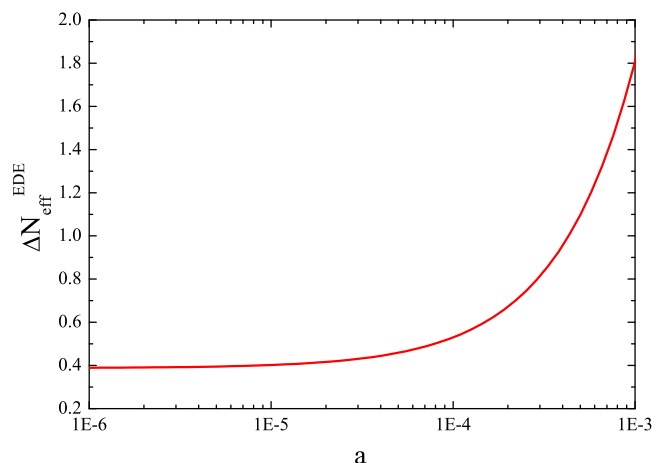


FIG. 1: Evolution of $\Delta N_{\text{eff}}^{\text{EDE}}$ as a function of the scale factor a , for $\Omega_e = 0.05$ (the results scale nearly linearly for smaller values). Note the strong time dependence near recombination.

C. Barotropic Dark Energy

As a model with some characteristics of each of the previous two, we consider a case containing dark radiation, that is a component whose energy density evolves as $\rho \propto a^{-4}$ but does not interact electromagnetically. Such terms arise in higher dimensional theories with multiple branes that induce a Weyl tensor contribution to the energy-momentum tensor [14]. Here we choose a more conventional model with interesting properties, arising

from the barotropic class [31] where the pressure is an explicit function of the energy density. Barotropic models were shown to be highly predictive, reducing the cosmological constant fine tuning problem by rapidly evolving through an attractor mechanism toward $w = -1$ [32]. Their equation of state, and hence energy density evolution, is wholly determined by their sound speed, through

$$w' \equiv dw/d\ln a = -3(1+w)(c_s^2 - w). \quad (7)$$

This gives for any constant c_s a time dependent equation of state

$$w = [c_s^2 B a^{-3(1+c_s^2)} - 1] / [B a^{-3(1+c_s^2)} + 1], \quad (8)$$

where $B = (1 + w_0)/(c_s^2 - w_0)$.

Being interested in relativistic degrees of freedom, we choose $c_s^2 = 1/3$ (and indeed $c_s^2 > 1/3$ would violate early radiation domination). This leads to a surprisingly simple solution:

$$\rho_{\text{baro}}(a) = \rho_\infty + C \rho_{r,0} a^{-4}, \quad (9)$$

where $\rho_\infty = (3H_0^2/8\pi G)(1 - \Omega_m - C\Omega_{r,0})$ and $C = \Omega_e^B/(1 - \Omega_e^B)$. This acts like radiation at early times, with a constant fractional energy density Ω_e^B during the radiation dominated era. At late times it has a constant absolute energy density ρ_∞ . It basically looks like the sum of a cosmological constant and dark radiation, despite having no explicit cosmological constant. As expected, at early times $w = 1/3$ and at late times w rapidly approaches -1 . We take $w_0 = -0.99$ (since $w = -1$ is only reached asymptotically), and $c_{vis}^2 = 1/3$ to match the other cases.

To clearly state the main practical differences of our three models: extra neutrino species give a constant contribution to N_{eff} and negligible contribution to late time energy density as well as no acceleration; standard early dark energy gives a time varying contribution to N_{eff} as well as late time energy density and acceleration; barotropic dark energy has the third interesting combination of properties, giving a constant contribution to N_{eff} but also late time energy density and acceleration. The interplay between these properties will allow each model to impact the observations in a distinctive manner.

In addition to approaching this model microphysically, through the class of barotropic models, one can obtain an equivalent result within k-essence [33] using the quadratic Lagrangian $\mathcal{L} = X_0 + cX^2$, where X is the kinetic energy and c , X_0 are constants.

Because for this model the relativistic scaling occurs so quickly (by $z > 5$), the ΔN_{eff}^B contribution in this case will be constant at and before recombination, like the neutrino model with $\Delta N_{\text{eff}}^B = 7.44 \Omega_e^B/(1 - \Omega_e^B)$ (see Eq. 6). However it has the late time change in equation of state that will affect large scale aspects of the CMB, and other cosmological probes, like the EDE model. Thus we expect the results to have aspects of each of the other two cases.

D. Effects of the new components

Since our main observational datasets are CMB anisotropies, it is useful to see the effects of sterile neutrinos, EDE and barotropic dark energy on the CMB anisotropy angular spectrum. In Figure 2 (top panel) we show the CMB temperature angular spectra for these 3 components assuming that they contribute at the level of one extra degree of freedom at BBN. As we can see, while sterile neutrinos and barotropic dark energy produce nearly identical angular spectra, EDE predicts a significantly different spectrum. This is clearly shown in the bottom panel of the same figure where we plot the isolated Integrated Sachs Wolfe (ISW) contribution for each case. As we can see, the main difference between a sterile neutrino and EDE comes from the ISW effect. This is mainly due to the time-dependence of the equation of state in the EDE component that tracks the dominant component at all epochs and increases the ISW signal on all angular scales. At the same time, we see that barotropic dark energy differs from a sterile neutrino in the increase in the ISW at large angular scales, due to the variation in the equation of state at small redshift in the barotropic component.

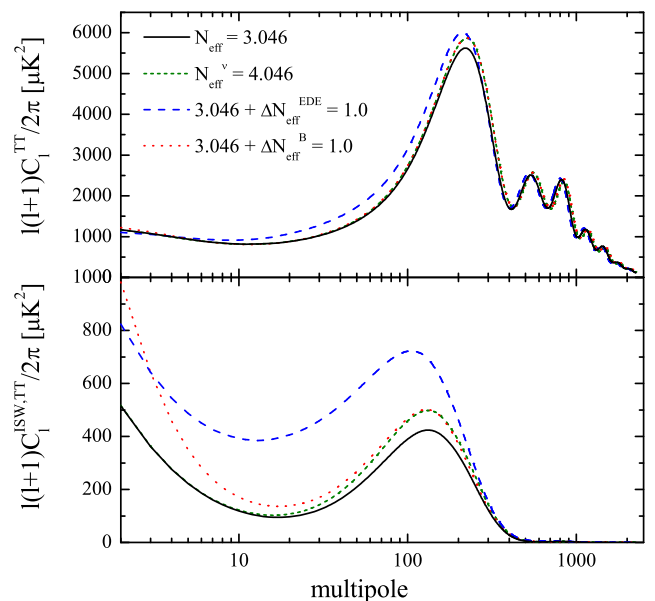


FIG. 2: CMB temperature (top panel) and ISW contribution alone (bottom panel) angular power spectra dependence from sterile neutrinos, early dark energy and barotropic dark energy. All the models have been chosen to produce one extra relativistic degree of freedom at the epoch of BBN, except for the solid curve showing the standard case.

III. ANALYSIS AND RESULTS

We perform a COSMOMC [34] analysis combining the following CMB datasets: WMAP7 [1], ACBAR [2], QUAD [3] (collectively referred to as “All”), and ACT [4]. We analyze datasets using out to $l_{\text{max}} = 2500$. We also include information on dark matter clustering from the galaxy power spectrum extracted from the SDSS-DR7 luminous red galaxy sample [35]. Finally, we impose a prior on the Hubble parameter based on the Hubble Space Telescope observations [36].

The analysis method we adopt is based on the publicly available Markov Chain Monte Carlo package `cosmomc` [37] with a convergence diagnostic done through the Gelman and Rubin statistic. We sample the following nine-dimensional set of cosmological parameters, adopting flat priors on them: the baryon and cold dark matter densities ω_b and ω_c , the Hubble constant H_0 , the scalar spectral index n_S , the overall normalization of the spectrum A at $k = 0.05 \text{ Mpc}^{-1}$, the SZ amplitude A_{SZ} , the optical depth to reionization, τ , the effective number of relativistic neutrinos N_{eff}^ν , and finally the early density Ω_e , for either the case of EDE or the barotropic model (Ω_e^B). For the ACT dataset we also consider two extra parameters accounting for the Poisson and clustering point sources foregrounds components. We consider purely adiabatic initial conditions and we impose spatial flatness.

To study the impact of EDE perturbations, we consider two cases: “quintessence” ($c_s^2 = 1, c_{\text{vis}}^2 = 0$) and “relativistic” ($c_s^2 = 1/3 = c_{\text{vis}}^2$) EDE scenarios. For the barotropic dark energy model we assume $c_s^2 = 1/3 = c_{\text{vis}}^2$.

A. Constraints on EDE with $N_{\text{eff}}^\nu = 3.046$ fixed

We first perform an analysis of current data fixing the effective number of relativistic neutrinos to the standard value of $N_{\text{eff}}^\nu = 3.046$ and varying the amount of early dark energy, parametrized as Ω_e . The EDE affects the CMB angular power spectrum at all multipoles as shown in Fig. 2. We convert the EDE into an equivalent additional relativistic species $\Delta N_{\text{eff}}^{\text{EDE}}$ and quote this parameter at the BBN epoch. We also recognize the fact that the changed expansion rate during the BBN, due to the presence of EDE, also alters the primordial Helium mass fraction Y_p , and show the effect of Ω_e on Y_p below.

The MCMC results on the cosmological parameters are reported in the first two columns of Table I.

As we can see, the cosmological data we consider do not provide evidence for an EDE component and significantly improve the bound [25], yielding a 95% c.l. upper limit of $\Omega_e < 0.043$ in case of a “relativistic” EDE with $c_s^2 = c_{\text{vis}}^2 = 1/3$, and a bound of $\Omega_e < 0.024$ in case of a “quintessence” EDE with $c_s^2 = 1, c_{\text{vis}}^2 = 0$. The assumptions of c_s and c_{vis} strongly affect the bounds on Ω_e . The “quintessence” scenario leaves a stronger signal on the CMB anisotropies (see e.g. [24]) and is therefore better constrained. This arises from the greater decay of

potentials at recombination in contrast to the low sound speed case where the dark energy perturbations help sustain the potentials.

In order to investigate the impact of the recent ACT dataset, which samples very small angular scales, giving a long lever arm, on the final result we also perform an analysis excluding it in the case of “relativistic” EDE. Without ACT we get a $\sim 20\%$ weaker bound, $\Omega_e < 0.051$ at 95% c.l..

While the EDE component is not preferred, it is also not excluded from current data. It is therefore interesting to investigate if the EDE component compatible with cosmological data is also compatible with BBN data. For this reason we translated the bounds on Ω_e into the corresponding bound on $\Delta N_{\text{eff}}^{\text{EDE}}$ expected at time of onset of BBN, using Eq. (6), and computed the expected abundance Y_p in primordial ^4He by making use of the public available PARthENoPE BBN code (see [38]). In other words, the constraints on early dark energy during the BBN correspond to limits on the expansion rate of the universe at this epoch, which translate into the corresponding limits on the excess of primordial mass fraction of Helium.

Table I shows the “relativistic” case 95% upper limit $\Omega_e < 0.043$ translates to a 95% constraint of $Y_p = 0.2504 \pm 0.0026$ (with $\Delta N_{\text{eff}}^{\text{EDE}} < 0.34$), while the “quintessence” case 95% upper limit $\Omega_e < 0.024$ translates to a 95% constraint of $Y_p = 0.2495 \pm 0.0016$ (with $\Delta N_{\text{eff}}^{\text{EDE}} < 0.18$). These values should be compared with the theoretical value of $Y_p = 0.2487 \pm 0.0002$ obtained assuming standard BBN and $\Omega_e = 0$. EDE is therefore clearly shifting the BBN predictions on Y_p towards larger values with weaker constraints. The weaker constraints indicate a degeneracy between Ω_e and Y_p , as we discuss more in the next section, that we also show in Figure 3 where we plot the 68% and 95% constraints on the Y_p - Ω_e plane in the case of “relativistic” or a “quintessence” EDE.

As stated in the introduction, current experimental measurements seems to prefer a larger value for the primordial Helium with $Y_p = 0.2561 \pm 0.0108$ (see [16]) or $Y_p = 0.2565 \pm 0.0010$ (stat.) ± 0.0050 (syst.) from [17]. These results are off by $\sim 1.5\sigma$ from the expectations of standard BBN but introducing EDE acts to alleviate this tension. Given the possibility of systematics in measuring the primordial nuclear abundances, however, it is premature to derive any conclusion.

B. Constraints on EDE and N_{eff}^ν

As a second step, we include into the analysis the possibility of extra sterile neutrinos, parametrizing it with the effective neutrino number N_{eff}^ν . As we can see from Table I (last two columns), the constraints on Ω_e are practically unaffected by the inclusion of extra RDOF and vice versa. From our analysis we found that sterile neutrinos are preferred with $N_{\text{eff}}^\nu = 4.37 \pm 0.76$ at 68%

	All+ACT			
Model:	$N_{\text{eff}}^\nu = 3.046$		N_{eff}^ν varying	
	$c_s^2 = c_{\text{vis}}^2 = 1/3$	$c_s^2 = 1, c_{\text{vis}}^2 = 0$	$c_s^2 = c_{\text{vis}}^2 = 1/3$	$c_s^2 = 1, c_{\text{vis}}^2 = 0$
Parameter				
$\Omega_b h^2$	0.02218 ± 0.00044	0.02232 ± 0.00044	0.02238 ± 0.00047	0.02259 ± 0.00048
$\Omega_c h^2$	0.1178 ± 0.0039	0.1163 ± 0.0038	0.138 ± 0.012	0.139 ± 0.011
H_0	68.2 ± 1.7	67.8 ± 1.6	72.5 ± 2.8	72.4 ± 2.7
n_s	0.971 ± 0.013	0.964 ± 0.011	0.988 ± 0.015	0.986 ± 0.015
t_0 / Gyr	13.71 ± 0.30	13.83 ± 0.29	12.91 ± 0.48	12.94 ± 0.48
N_{eff}^ν	3.046	3.046	4.37 ± 0.76	4.49 ± 0.72
Ω_e	< 0.043	< 0.024	< 0.039	< 0.020
$\Delta N_{\text{eff}}^{\text{EDE}}(a_{\text{BBN}})$	< 0.34	< 0.18	< 0.32	< 0.18
Y_p	0.2504 ± 0.0013	0.2495 ± 0.0008	0.2661 ± 0.0078	0.2667 ± 0.0080

TABLE I: Best-fit values and 68% confidence errors on cosmological parameters using the current cosmological data. For Ω_e and $\Delta N_{\text{eff}}^{\text{EDE}}(a_{\text{BBN}})$, EDE density and the contribution to the RDOF from EDE at the BBN epoch respectively, the upper bounds at 95% c.l. are reported. See text for other details.

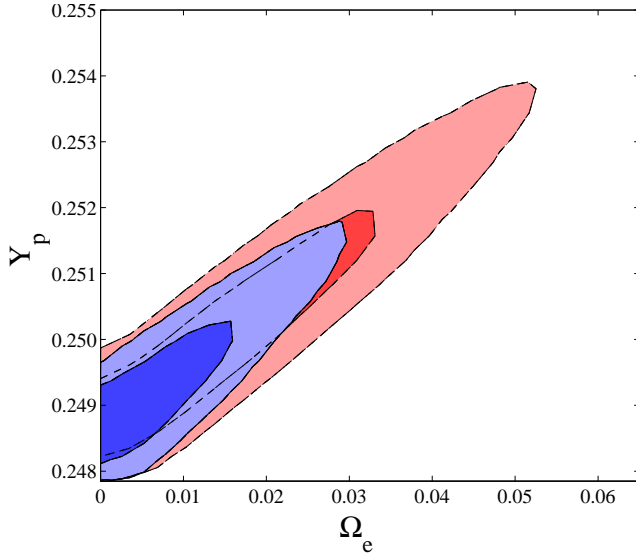


FIG. 3: 68% and 95% c.l. contours in the Y_p - Ω_e plane for the standard EDE model. The red dashed contours show the $c_s^2 = c_{\text{vis}}^2 = 1/3$ model, while the blue solid contours show the $c_s^2 = 1, c_{\text{vis}}^2 = 0$ model. Since the early dark energy enhances the expansion rate during the BBN, it allows for a higher primordial Helium mass fraction according to $\Delta Y_p \simeq 0.013(N_{\text{eff}} - 3)$ [18].

c.l.. This constraint should be compared with the bound from the analysis of [4] of $N_{\text{eff}}^\nu = 4.6 \pm 0.8$ at 68% c.l., obtained with similar datasets but without EDE, indicating that the effect of EDE on the constraint is small. The low covariance between the number of sterile neutrinos and EDE density comes from the property that while at BBN they both act as RDOF, by recombination the

EDE behaves more like matter and so can be constrained separately from the neutrino contribution.

This can also be seen in Figure 4 where we show the likelihood contour plots in the N_{eff}^ν - Ω_e plane for the cases of “relativistic” and “quintessence” EDE. There is no strong degeneracy between Ω_e and N_{eff}^ν . This, together with the small value of $\Delta N_{\text{eff}}^{\text{EDE}}$ allowed, indicates that the current hints for the existence of the extra RDOF cannot be completely explained by a conventional EDE model. In the next subsection we will see that the barotropic class of early dark energy has more success.

As we can see from Table I, including the possibility of extra neutrino contributions to N_{eff} greatly enlarges the CMB bounds on primordial Helium, with $Y_p = 0.2661 \pm 0.0078$ in case of “relativistic” EDE to $Y_p = 0.2667 \pm 0.0080$ in case of “quintessence” EDE. This stronger influence of neutrino RDOF than EDE has the consequence that in this situation the impact of EDE on the Y_p abundance is small. As seen from the results in Table I, the $\Delta N_{\text{eff}}^{\text{EDE}}$ from EDE at BBN is always better constrained from CMB data than the N_{eff}^ν expected from a sterile neutrino. If future measurements of primordial ^4He clearly point towards value of $Y_p \sim 0.26$, it will not be possible to explain this result with a conventional EDE contribution.

Finally, we note that including the possibility of $N_{\text{eff}}^\nu > 3$ also changes the constraints on n_s making it more compatible with a Harrison-Zeldovich, $n_s = 1$, primordial spectrum (cf. [30, 39]). The best fit value of the inflationary tilt $n_s - 1$ is reduced by almost a factor of 3, which would have a substantial impact in the reconstruction of the inflationary potential.

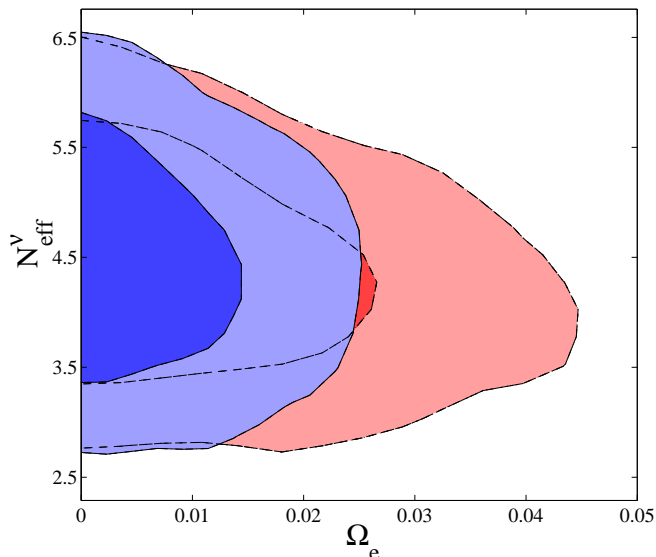


FIG. 4: 68% and 95% c.l. contours in the N_{eff}^{ν} - Ω_e plane for the standard EDE model plus neutrinos). The red dashed contours refer to $c_s^2 = c_{\text{vis}}^2 = 1/3$ case, while the blue solid contours refer to the $c_s^2 = 1, c_{\text{vis}}^2 = 0$ case.

C. Results on Barotropic Dark Energy

The barotropic model contributes both early dark energy density and a constant (rather than diluted as in Fig. 1) early time RDOF. This will have interesting implications. As for the conventional EDE case, we add the early density, here Ω_e^B , to the MCMC analysis to estimate constraints on cosmological parameters. We also allow N_{eff}^{ν} to vary as in the previous section. For simplicity, we otherwise fix $w_0 = -0.99$ and $c_s^2 = c_{\text{vis}}^2 = 1/3$. The results are reported in Table II, and in Figure 5 we show the degeneracy between N_{eff}^{ν} and Ω_e^B parameters.

The barotropic model strongly alters the constraints on N_{eff}^{ν} and a non-negligible presence of the dark radiation part of the barotropic dark energy at recombination could not only bring the constraints on N_{eff}^{ν} back in agreement with the standard value of $N_{\text{eff}}^{\nu} = 3.046$ but even erase the current claim for a neutrino background from CMB data. A “neutrinoless” model with $N_{\text{eff}}^{\nu} = 0$ and $\Omega_e^B = 0.4$, albeit extreme, is allowed by the cosmological data we consider here.

As in the case for $N_{\text{eff}}^{\nu} > 3$, when a barotropic dark energy model is considered (even without extra neutrinos) a high value of Y_p is consistent and the constraints on n_s are moved toward a Harrison-Zeldovich primordial spectrum.

D. Forecasts for the Planck Satellite Mission

Looking to the future, we investigate the constraints on EDE and RDOF in the case of the data as expected from the Planck satellite. To evaluate the future constraints

Parameter	All + ACT
$\Omega_b h^2$	0.02209 ± 0.00055
$\Omega_c h^2$	0.135 ± 0.012
H_0	71.1 ± 2.8
n_s	0.986 ± 0.015
t_0 / Gyr	13.18 ± 0.51
N_{eff}^{ν}	< 5.1
Ω_e^B	< 0.37
ΔN_{eff}^B	< 2.8
Y_p	0.2649 ± 0.0084

TABLE II: Best-fit values, together with 68% confidence errors, on cosmological parameters for the barotropic model using current data. For the N_{eff}^{ν} , Ω_e^B and ΔN_{eff}^B parameters upper bound at 95% c.l. are reported.

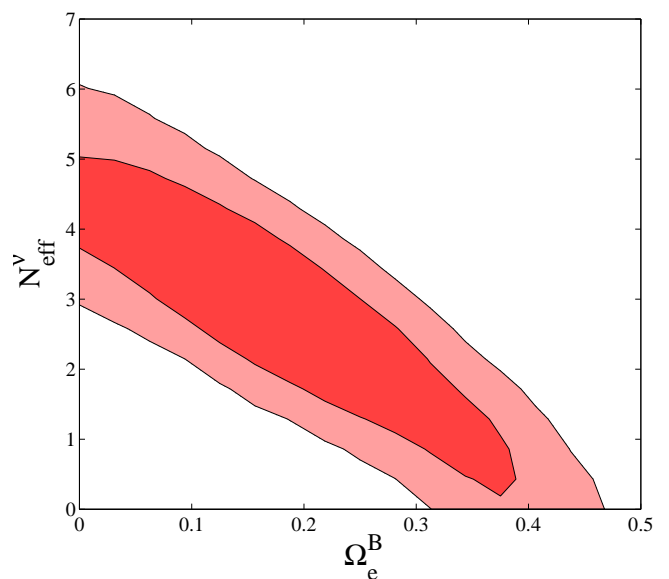


FIG. 5: 68% and 95% c.l. contours in the N_{eff}^{ν} - Ω_e^B plane for the barotropic dark energy model.

achievable from this satellite, we consider an experimental configuration with three frequency channels with the specifications as listed in Table III (see [40]).

Experiment	Channel[GHz]	FWHM	$\sigma_T[\mu K]$	$\sigma_P[\mu K]$
Planck	143	7.1'	6.0	11.4
$f_{\text{sky}} = 0.85$	100	10.0'	6.8	10.9
	70	14.0'	12.8	18.3

TABLE III: Planck experimental specifications.

For each frequency channel we consider a detector noise of $(\theta\sigma)^2$ where θ is the FWHM of the beam assuming a Gaussian profile and σ is the sensitivity. We therefore

take a noise spectrum given by

$$N_\ell^X = (\theta\sigma_X)^2 e^{l(l+1)/l_b^2}, \quad (10)$$

where $l_b \equiv \sqrt{8\ln 2}/\theta$ and the label X refers to either temperature or polarization, $X = T, P$.

We perform the standard Fisher matrix analysis evaluating (see e.g. [41]):

$$F_{ij} \equiv \left\langle -\frac{\partial^2 \ln \mathcal{L}}{\partial p_i \partial p_j} \right\rangle_{p_0}, \quad (11)$$

where $\mathcal{L}(\text{data}|\mathbf{p})$ is the likelihood function of a set of parameters \mathbf{p} given some data, and the partial derivatives and the averaging are evaluated using the fiducial values \mathbf{p}_0 of the parameters. The Cramér-Rao inequality implies that $(F^{-1})_{ii}$ is the smallest variance in the parameter p_i , so we can generally think of F^{-1} as the best possible covariance matrix for estimates of the vector \mathbf{p} . The one sigma error forecasted for each parameter is then given by $\sigma_{p_i} = \sqrt{(F^{-1})_{ii}}$.

We consider a set of 10 cosmological parameters with the following fiducial values: the physical baryonic and cold dark matter densities relative to critical $\Omega_b h^2 = 0.02258$ and $\Omega_c h^2 = 0.1109$, the optical depth to reionization $\tau = 0.088$, the Hubble parameter $H_0 = 71$ km/s/ Mpc, the current dark energy equation of state $w_0 = -0.95$, the early dark energy density relative to critical $\Omega_e = 0.03$, the spectral index $n_s = 0.963$, and the number of relativistic neutrinos $N_{\text{eff}} = 3.046$. For the last two parameters, the effective and viscous sound speeds c_s^2 and c_{vis}^2 , we choose alternate fiducial values of $(1/3, 1/3)$ (the “relativistic” model) or $(1, 0)$ (the “quintessence” model).

1. EDE Forecasts

In Table IV we report the uncertainties obtained on the cosmological parameters. The degeneracy between Ω_e and N_{eff}^ν is shown in Figure 6 for the two analysed cases. As seen in the Figure and in the Table, the future data from Planck will provide strong constraints on the RDOF: $\sigma(N_{\text{eff}}) = 0.11$, with little impact from the EDE density. If EDE with $\Omega_e = 0.03$ is present, it will be detected at high significance, since $\sigma(\Omega_e) \approx 0.005$. The radiation and quintessence configurations of EDE can also be distinguished.

2. Barotropic DE Forecasts

Similarly to the previous analysis, we forecasted the errors on cosmological parameters with data expected from Planck in a barotropic dark energy scenario. We report in Table V the $1-\sigma$ errors, and in Figure 7 we show the degeneracy between N_{eff}^ν and Ω_e^B .

For a fiducial early density of $\Omega_e^B = 0.03$, the barotropic model cannot be readily distinguished from the standard EDE model. However, if Ω_e^B is

		Planck 1- σ uncertainty	
Model:		$c_s^2 = c_{\text{vis}}^2 = 1/3$	$c_s^2 = 1, c_{\text{vis}}^2 = 0$
Parameter	Fiducial		
$\Omega_b h^2$	0.02258	0.00016	0.00014
$\Omega_c h^2$	0.1109	0.0018	0.0017
τ	0.0880	0.0020	0.0022
H_0	71.0	8.5	8.8
n_s	0.9630	0.0046	0.0044
N_{eff}^ν	3.046	0.11	0.11
w_0	-0.95	0.24	0.24
Ω_e	0.030	0.005	0.004
c_s^2	0.33	0.047	—
c_{vis}^2	0.33	0.13	—
c_s^2	1.00	—	0.34
c_{vis}^2	0	—	0.11

TABLE IV: Fiducial errors and forecasted 1- σ errors expected from the Planck satellite in the EDE scenario.

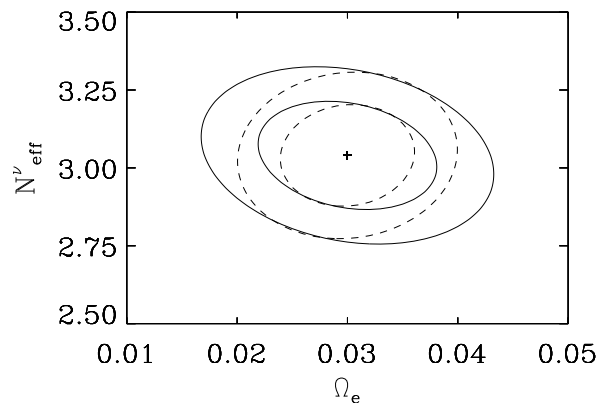


FIG. 6: 68% and 95% c.l. constraints in the N_{eff}^ν - Ω_e plane. Solid lines show the “relativistic” case $c_s^2 = c_{\text{vis}}^2 = 1/3$, while dashed lines show the “quintessence” case $c_s^2 = 1, c_{\text{vis}}^2 = 0$. The fiducial values are given by the “+” symbol.

much larger, then distinction will be possible, with the associated implications for RDOF, Y_p , and n_s .

IV. CONCLUSIONS

Data analyses of recent cosmological data have reported an interesting indication for the presence of an extra background of relativistic particles. In this paper we have investigated the stability of this result by considering the influence of a possible early dark energy component. We have found that current data do not provide evidence for an EDE component, updating and strengthening previous constraints on EDE, although there is still room for an interesting contribution. In particular, we

		Planck 1- σ uncertainty
Model:		$c_s^2 = c_{\text{vis}}^2 = 1/3$
Parameter	Fiducial	
$\Omega_b h^2$	0.02258	0.00013
$\Omega_c h^2$	0.1109	0.0019
τ	0.0880	0.0022
H_0	71.00	0.88
n_s	0.9630	0.0041
N_{eff}^ν	3.046	0.17
w_0	-0.95	0.041
Ω_e^B	0.030	0.015
c_s^2	0.33	0.045
c_{vis}^2	0.33	0.17

TABLE V: Same as Table IV, but for the barotropic dark energy scenario.

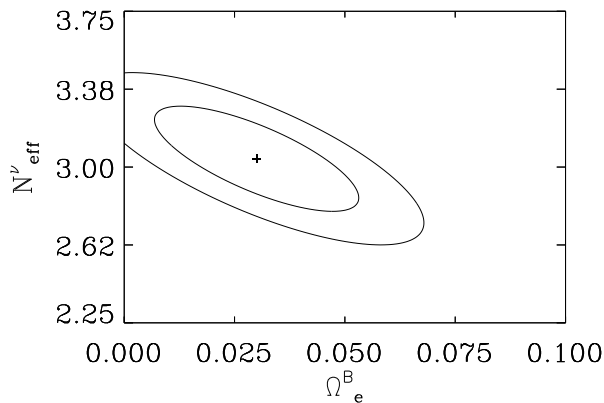


FIG. 7: 2-D contour plots at 68% and 95% c.l. in the plane N_{eff}^ν - Ω_e^B for $c_s^2 = c_{\text{vis}}^2 = 1/3$. The fiducial values are reported with the “+” symbol.

found the following 95% c.l. upper limits: $\Omega_e < 0.043$ for “relativistic” EDE ($c_s^2 = c_{\text{vis}}^2 = 1/3$) and $\Omega_e < 0.024$ for “quintessence” EDE ($c_s^2 = 1$, $c_{\text{vis}}^2 = 0$). These bounds translate into an extra relativistic background at BBN of $\Delta N_{\text{eff}}^{EDE} < 0.34$ and $\Delta N_{\text{eff}}^{EDE} < 0.18$ at 95% c.l., respectively.

The EDE models are therefore not able to change the amount of primordial ^4He produced in BBN by more than $\Delta Y_P^{EDE} = 0.0044$, and do not help much in explaining why recent measurements of abundances of primordial Helium show values larger than those expected from standard BBN. The systematics in those measurements are however still too large to conclude that there is conflict between the measured and predicted ^4He abundance.

When *both* an EDE and extra sterile neutrinos are considered in the analysis, there is very little degener-

acy between them and the constraints are virtually unaffected. The indication for extra neutrinos in current data at about two standard deviations is unchanged even after allowing a EDE component. We found $N_{\text{eff}}^\nu = 4.37 \pm 0.75$ at 68% c.l. for relativistic EDE and $N_{\text{eff}}^\nu = 4.49 \pm 0.72$ for quintessence EDE when CMB, SDSS-DR7 and HST data are combined. The bounds on Ω_e are practically unchanged. The key point is that EDE starts to behave differently from a relativistic component after radiation-matter equality, before the epoch of recombination. CMB data can therefore provide crucial information in discriminating between N_{eff}^ν and early dark energy while for BBN these two components are virtually indistinguishable.

However, when a barotropic dark energy model is considered, we have found that the constraints on N_{eff}^ν can be strongly altered, bringing the standard value of $N_{\text{eff}}^\nu = 3.046$ back into perfect agreement with observations. In fact, even a “neutrinoless” model with $N_{\text{eff}}^\nu = 0$ and $\Omega_e^B = 0.4$ is allowed given current observations. While that is extreme, the model dependency clearly indicates the caveats of considering $N_{\text{eff}}^\nu > 3.046$ as an indication for an extra sterile neutrino or claiming any detection for a neutrino background. Interestingly, barotropic dark energy also shifts Y_p to higher values, and reduces $|n_s - 1|$, with implications for models of inflation.

Finally, we have shown that for the Planck experiment alone, again no substantial degeneracy is expected between Ω_e and N_{eff}^ν , with an expected accuracy of $\sigma(N_{\text{eff}}^\nu) = 0.11$ and $\sigma(\Omega_e) = 0.005$. However, in a barotropic dark energy scenario the degeneracy is present and Planck will offer weaker bounds with an estimated $\sigma(N_{\text{eff}}^\nu) = 0.17$ and $\sigma(\Omega_e^B) = 0.015$. Both are still a great improvement over present data. Planck will therefore shed light on various scenarios for early dark energy and relativistic degrees of freedom, exploring if new physics exists in the neutrino or dark energy sectors, a possible shift in the inflationary tilt $n_s - 1$, and the consistency of the primordial Helium abundance Y_p .

Acknowledgments

EC and AM are supported by PRIN-INAF grant, “Astronomy probes fundamental physics”. DH is supported by the DOE OJI grant under contract DE-FG02-95ER40899, NSF under contract AST-0807564, and NASA under contract NNX09AC89G. EL has been supported in part by the World Class University grant R32-2009-000-10130-0 through the National Research Foundation, Ministry of Education, Science and Technology of Korea and also by the Director, Office of Science, Office of High Energy Physics, of the U.S. Department of Energy under Contract No. DE-AC02-05CH11231; he thanks Nordita for hospitality during part of this work, and Claudia de Rham for helpful discussions.

-
- [1] E. Komatsu *et al.*, arXiv:1001.4538 [astro-ph.CO].
 - [2] C. L. Reichardt *et al.*, *Astrophys. J.* **694** (2009) 1200 [arXiv:0801.1491 [astro-ph]].
 - [3] S. Gupta *et al.* [QUaD collaboration], arXiv:0909.1621 [astro-ph.CO].
 - [4] J. Dunkley *et al.*, arXiv:1009.0866 [astro-ph.CO].
 - [5] J. Hamann, S. Hannestad, G. G. Raffelt, I. Tamborra and Y. Y. Y. Wong, *Phys. Rev. Lett.* **105** (2010) 181301 [arXiv:1006.5276 [hep-ph]].
 - [6] G. Mangano, A. Melchiorri, O. Mena, G. Miele and A. Slosar, *JCAP* **0703**, 006 (2007) [arXiv:astro-ph/0612150].
 - [7] U. Seljak, A. Slosar and P. McDonald, *JCAP* **0610** (2006) 014 [arXiv:astro-ph/0604335].
 - [8] L. Zhang, X. Chen, M. Kamionkowski, Z. g. Si and Z. Zheng, *Phys. Rev. D* **76** (2007) 061301 [arXiv:0704.2444 [astro-ph]].
 - [9] J. Chluba and R. A. Sunyaev, *A & A* **501**, 29-47 (2009) [arXiv:0803.3584 [astro-ph]].
 - [10] W. Fischler and J. Meyers, arXiv:1011.3501 [astro-ph.CO].
 - [11] S. Bashinsky and U. Seljak, *Phys. Rev. D* **69** (2004) 083002 [arXiv:astro-ph/0310198].
 - [12] P. G. Ferreira and M. Joyce, *Phys. Rev. D* **58** (1998) 023503 [arXiv:astro-ph/9711102].
 - [13] A. R. Liddle and R. J. Scherrer, *Phys. Rev. D* **59** (1999) 023509 [arXiv:astro-ph/9809272].
 - [14] P. Binetruy, C. Deffayet, U. Ellwanger and D. Langlois, *Phys. Lett. B* **477** (2000) 285 [arXiv:hep-th/9910219].
 - [15] L. M. Krauss, C. Lunardini and C. Smith, arXiv:1009.4666 [hep-ph].
 - [16] E. Aver, K. A. Olive and E. D. Skillman, *JCAP* **1005** (2010) 003 [arXiv:1001.5218 [astro-ph.CO]].
 - [17] Y. I. Izotov and T. X. Thuan, *Astrophys. J.* **710**, L67 (2010) [arXiv:1001.4440 [astro-ph.CO]].
 - [18] G. Steigman, *JCAP* **1004** (2010) 029. [arXiv:1002.3604 [astro-ph.CO]].
 - [19] P. C. de Holanda and A. Y. Smirnov, arXiv:1012.5627 [hep-ph].
 - [20] E. Akhmedov and T. Schwetz, *JHEP* **1010** (2010) 115 [arXiv:1007.4171 [hep-ph]].
 - [21] C. Giunti and M. Laveder, *Phys. Rev. D* **82** (2010) 053005 [arXiv:1005.4599 [hep-ph]].
 - [22] M. Doran and G. Robbers, *JCAP* **0606** (2006) 026 [arXiv:astro-ph/0601544].
 - [23] E. V. Linder and G. Robbers, *JCAP* **0806** (2008) 004 [arXiv:0803.2877 [astro-ph]].
 - [24] E. Calabrese, R. de Putter, D. Huterer, E. V. Linder and A. Melchiorri, *Phys. Rev. D* **83** (2011) 023011 [arXiv:1010.5612 [astro-ph.CO]].
 - [25] R. de Putter, D. Huterer and E. V. Linder, *Phys. Rev. D* **81** (2010) 103513 [arXiv:1002.1311 [astro-ph.CO]].
 - [26] U. Alam, Z. Lukic and S. Bhattacharya, arXiv:1004.0437 [astro-ph.CO].
 - [27] L. Hollenstein, D. Sapone, R. Crittenden and B. M. Schaefer, *JCAP* **0904** (2009) 012 [arXiv:0902.1494 [astro-ph.CO]].
 - [28] J. Q. Xia and M. Viel, *JCAP* **0904** (2009) 002 [arXiv:0901.0605 [astro-ph.CO]].
 - [29] E. Giusarma, M. Corsi, M. Archidiacono, R. de Putter, A. Melchiorri, O. Mena and S. Pandolfi, arXiv:1102.4774 [astro-ph.CO].
 - [30] S. Galli, R. Bean, A. Melchiorri and J. Silk, *Phys. Rev. D* **78** (2008) 063532 [arXiv:0807.1420 [astro-ph]].
 - [31] R. J. Scherrer, *Phys. Rev. D* **73** (2006) 043502 [arXiv:astro-ph/0509890].
 - [32] E. V. Linder and R. J. Scherrer, *Phys. Rev. D* **80** (2009) 023008 [arXiv:0811.2797 [astro-ph]].
 - [33] R. J. Scherrer, *Phys. Rev. Lett.* **93** (2004) 011301 [arXiv:astro-ph/0402316].
 - [34] A. Lewis, A. Challinor and A. Lasenby, *Astrophys. J.* **538** (2000) 473 [arXiv:astro-ph/9911177].
 - [35] B. A. Reid *et al.*, *Mon. Not. Roy. Astron. Soc.* **404** (2010) 60 [arXiv:0907.1659 [astro-ph.CO]].
 - [36] A. G. Riess *et al.*, *Astrophys. J.* **699**, 539 (2009) [arXiv:0905.0695 [astro-ph.CO]].
 - [37] A. Lewis and S. Bridle, *Phys. Rev. D* **66**, 103511 (2002) (Available from <http://cosmologist.info>.)
 - [38] O. Pisanti, A. Cirillo, S. Esposito, F. Iocco, G. Mangano, G. Miele and P. D. Serpico, *Comput. Phys. Commun.* **178**, 956 (2008) [arXiv:0705.0290 [astro-ph]].
 - [39] F. De Bernardis, R. Bean, S. Galli, A. Melchiorri, J. I. Silk and L. Verde, *Phys. Rev. D* **79** (2009) 043503 [arXiv:0812.3557 [astro-ph]].
 - [40] [Planck Collaboration], arXiv:astro-ph/0604069.
 - [41] J. R. Bond, G. Efsthathiou and M. Tegmark, *Mon. Not. Roy. Astron. Soc.* **291** (1997) L33 [arXiv:astro-ph/9702100].